

1 **Frozen Storage of Proteins: Use of Mannitol to Generate a Homogenous Freeze-**
2 **concentrate**

3
4 Jayesh Sonje^{a,1}, Carly Fleagle Chisholm^b and Raj Suryanarayanan^a
5
6

7 ^a Department of Pharmaceutics, College of Pharmacy, 308 Harvard St. SE,
8 University of Minnesota, Minneapolis, MN 55455, USA

9 ^b Drug Product Development, BioTherapeutics Development & Supply, Janssen Research &
10 Development, Malvern, PA 19355, USA

11
12
13
14
15 *Correspondence to:* Raj Suryanarayanan, PhD

16 Telephone: (612) 624-9626 Fax: (612) 626-2125

17 Email: surya001@umn.edu

18

19

¹ Current affiliation: Pfizer Biotherapeutics, Pfizer Inc., Andover, MA 01810, USA

20 **ABSTRACT**

21 Therapeutic proteins may be subjected to several freeze-thaw cycles throughout manufacturing
22 and storage. The protein solution composition and the freezing conditions may lead to incomplete
23 ice crystallization in the frozen state. This can also result in freeze-concentrate heterogeneity
24 characterized by multiple glass transition temperatures and protein destabilization. The overall
25 objective was to investigate the potential advantages of including a crystallizing excipient
26 (mannitol) along with a sugar (sucrose or trehalose) for frozen storage. This study showed that the
27 addition of mannitol, a readily crystallizing excipient, facilitated ice crystallization. Inclusion of
28 an isothermal hold during cooling (annealing) maximized the mannitol crystallization and resulted
29 in a homogenous freeze-concentrate of a constant composition characterized by a single glass
30 transition temperature. The role of freezing rate and annealing on both mannitol and ice
31 crystallization were discerned using high intensity synchrotron radiation. The addition of sucrose
32 or trehalose, at an appropriate concentration, stabilized the protein. The mannitol to sugar ratio
33 (3:1 or 1:1, 5% w/v) was optimized to selectively cause maximal crystallization of mannitol while
34 retaining the sugar amorphous. Human serum albumin (1 mg/mL) in these optimized and annealed
35 compositions did not show any meaningful aggregation, even after multiple freeze-thaw cycles.
36 Thus, in addition to a sugar as a stabilizer, the use of a crystallizing excipient coupled with an
37 annealing step can provide an avenue for frozen storage of proteins.

38 **Keywords:** Homogenous freeze-concentrate, matrix, mannitol, sucrose, trehalose, frozen storage,
39 freeze-thaw, protein

40

41 **1. INTRODUCTION**
42

43 Manufacturing of macromolecules is often divided into two steps – Drug Substance (DS) and Drug
44 Product (DP) manufacturing. The DS is often stored in the frozen state and thawed for DP
45 manufacturing. Occasionally, intermediate solutions and drug product (DP) are also stored frozen
46 (Rathore and Rajan, 2008). The frozen state substantially enhances the shelf life of the DS by
47 minimizing its mobility and hence slowing down reaction rates. It also reduces the risk of microbial
48 growth and helps overcome transport-related stress (e.g. shaking, agitation etc.) (Kolhe and
49 Badkar, 2011; Singh et al., 2009). However, destabilization of macromolecules can occur during
50 freezing and thawing and freeze-thaw related issues can be challenging to overcome. Successful
51 frozen storage of macromolecules requires careful consideration of the biophysical principles
52 dictating stability (Singh et al., 2009).

53 Protein formulations commonly contain several excipients including a buffer, a sugar or sugar-
54 alcohol, and a surfactant to prevent protein degradation which can occur through various
55 mechanisms. Freeze concentration or cold denaturation induced aggregation remains of concern
56 during freezing and frozen storage (Arsiccio and Pisano, 2020; Authelin et al., 2020). Freezing is
57 initiated by ice nucleation followed by ice crystal growth. Due to supercooling, ice nucleation is
58 often observed substantially below the equilibrium freezing point (Carpenter et al., 1997). Most of
59 the water then separates into ice crystals. The excipient (also referred to as solute) may either
60 crystallize or be retained as a freeze-concentrate. Ice formation is influenced by numerous factors
61 including shelf temperature, freezing ~~and thawing~~ rate, formulation composition and
62 concentration, as well as container shape and size. Once ice nucleates, crystallization and phase
63 separation of the ice continues until a maximally freeze concentrated solution is achieved
64 (assuming the solute is retained amorphous). During the freezing process, proteins are exposed to

65 stresses including adsorption at the ice-water interface , pH changes due to freeze-concentration
66 and phase separation causing unequal distribution of the stabilizer and protein (Bhatnagar et al.,
67 2007; Connolly et al., 2015; Piedmonte et al., 2007). The cooling rate and the type and
68 concentration of excipients are important factors governing protein stability.

69 The role of stabilizers (also referred to as cryoprotectants) is to prevent protein denaturation
70 including aggregation during processing and storage. Non-crystallizing excipients (stabilizers) are
71 known to prevent protein denaturation by preferential exclusion and viscous glass formation
72 (Chang and Pikal, 2009). The most important role of these stabilizers is to prevent the unfolding
73 of the protein both during freezing and thawing. According to the preferential exclusion
74 mechanism, the amorphous excipient is selectively excluded from the immediate vicinity of the
75 protein surface thereby enabling its stabilization in the native state. A second mechanism is the
76 decrease in protein mobility brought about by the increase in viscosity of the freeze-concentrate
77 (Wang, 2005). In order to exert their protective action, these stabilizers should remain amorphous.

78 When a solution containing a crystallizing solute is cooled, at the eutectic temperature, complete
79 crystallization of the solute and ice should ideally occur. However, most of the solutes used in
80 protein formulations do not crystallize readily when frozen. When a solute is retained amorphous,
81 an important attribute of the frozen system is the glass transition temperature of the freeze-
82 concentrate (T_g'). Stabilizers used in protein formulations including sugars, surfactants, and amino
83 acids contribute to formation of an amorphous matrix. Their utility comes from their ability to
84 remain amorphous with the protein in the freeze concentrated phase. Ideally, storage of the frozen
85 mass in the deeply glassy state, for example at approximately 50°C below the glass transition
86 temperature ($T_g' - 50$), is assumed to inhibit mobility sufficiently to prevent mobility-induced
87 protein degradation or excipient crystallization (Hancock and Zografi, 1997). However, given the

88 nature of supply chain logistics, it can be challenging to store the frozen bulk at very low
89 temperatures. There are examples of several systems stored at -70°C which can be practically
90 difficult, expensive, and pose significant challenges with maintaining the cold chain. The freeze-
91 concentrate composition dictates the Tg' and decreases with an increase in unfrozen water content.
92 From a processing and storage perspective, we desire compositions with the highest possible Tg'
93 to avoid the need for storage at very low temperatures.

94 Sugars such as trehalose and sucrose are used as stabilizers in protein solutions due to their ability
95 to serve as cryoprotectants and resist crystallization. In lyophilized formulations, a combination
96 of stabilizer and a bulking agent has been used as a successful strategy to prevent protein
97 aggregation as well as provide necessary mechanical strength to the final cake (Johnson et al.,
98 2002). Mannitol, a popular bulking agent, has been used due its high propensity to crystallize
99 during freezing along with its high eutectic melting temperature which results in short drying
100 cycles (Kim et al., 1998). Sucrose-mannitol-water ternary solutions exhibit two Tg' (~ -48 and -
101 34°C) during freezing. The multiple Tg' values reflect heterogeneity in the freeze concentrate. The
102 composition with a lower glass transition temperature has a higher amount of unfrozen water
103 ("water rich" phase) while the composition with the higher glass transition temperature is a "solute
104 rich" phase). However, irrespective of composition and processing (annealing), sucrose is
105 consistently retained in the amorphous state. Annealing is typically conducted to facilitate solute
106 crystallization in frozen systems (Searles et al., 2001). In ternary mannitol-sucrose-water systems,
107 complete mannitol crystallization, and hence its phase separation, will result in a frozen matrix
108 which will resemble sucrose-water binary system. Since mannitol has a strong propensity to
109 crystallize, this can be achieved with the judicious selection of processing steps.

110 Trehalose-mannitol-water ternary solutions also exhibit two T_g' (~ -45 and -32°C) reflecting
111 heterogeneity in the freeze concentrate. Investigation of different weight ratios of mannitol to
112 trehalose (R) revealed that when R=1, at annealing temperatures higher than T_g' , mannitol
113 crystallization led to trehalose crystallization, whereas at R = 3 only mannitol crystallized (Jena et
114 al., 2017). Crystallization of trehalose may compromise its cryoprotectant function. Connolly et
115 al. investigated the impact of cooling rate, storage temperature, and formulation composition on
116 mAb aggregation in the presence of trehalose during lyophilization. The trehalose crystallization
117 in this case was ensured either by seeding or by controlled ice nucleation. The mAb showed highest
118 aggregation after 12-months storage at a temperature of -20°C as opposed to no aggregation in
119 samples stored at -40°C. The study highlights that if the storage temperature is below the T_g' of
120 the frozen matrix, protein aggregation can be significantly prevented (Connolly et al., 2015).
121 Furthermore, it is necessary to identify trehalose to mannitol ratios which will lead to selective
122 crystallization of only mannitol and not trehalose. It is also instructive to recognize that the protein,
123 in a concentration dependent manner, will inhibit the crystallization of both trehalose and mannitol.
124 The process parameters for annealing may be designed to promote the crystallization of only
125 mannitol.

126 In ternary mannitol-sugar-water systems, substantial if not complete mannitol phase separation
127 (crystallization) can be accomplished if it is initiated early in the freezing process. Complete
128 mannitol phase separation (crystallization) in a frozen matrix is a desirable attribute. Mannitol
129 crystallization will also result in the crystallization of the associated unfrozen water. This has the
130 potential to reduce the phase separation. We hypothesize that in frozen systems, mannitol
131 crystallization *during* freezing can result in a homogeneous freeze concentrate (characterized by a
132 single T_g'). Complete mannitol crystallization can be accomplished by (i) annealing the solution

133 during cooling and (ii) using specific mannitol to sugar ratios. In other words, the goal of our work
134 was to use a crystallizing excipient to promote ice crystallization and obtain a freeze-concentrate
135 of consistent and constant composition. Baseline thermal characterization of mannitol-sucrose and
136 mannitol-trehalose mixtures of different compositions was performed using DSC. In order to
137 identify the phases crystallizing from solution, *in situ* (during cooling as well as heating) low
138 temperature X-ray diffractometric measurements (synchrotron source) was performed. To achieve
139 maximum mannitol and ice crystallization, process conditions including (i) cooling at slow rates,
140 and (ii) isothermally holding the optimized mannitol-sugar compositions at desired subambient
141 temperatures during cooling were investigated. In the context of this work, we refer to the
142 isothermal hold during cooling step as ‘annealing’. Human serum albumin (HSA) was the model
143 protein used in this study. Aggregation of HSA in solutions that contained histidine, mannitol, and
144 either sucrose or trehalose was monitored by SE-HPLC after multiple freeze-thaw cycles.

145

146 **2. MATERIALS AND METHODS**

147

148 ***2.1. Materials***

149 Mannitol ($C_6H_{14}O_6$), sucrose ($C_{12}H_{22}O_{11}$), trehalose ($C_{12}H_{22}O_{11}$), L-histidine, histidine
150 monohydrochloride and human serum albumin (HSA, $\geq 99.0\%$ purified) were purchased from
151 Sigma-Aldrich (St. Louis, MO, USA). Aqueous solutions of mannitol and either sucrose or
152 trehalose were prepared in 1:1, 2:1 and 3:1 ratio with a total solute concentration of 5% w/v in 10
153 mM histidine buffer solutions.

154 ***2.2. Differential Scanning Calorimetry (DSC)***

155 A differential scanning calorimeter (model Q2000 TA instruments, New Castle, DE, USA)
156 equipped with a cooling system was used. The instrument was calibrated with tin and indium. Dry

157 nitrogen at 50 mL/min was used as the purge gas. In the first set of studies, approximately 15 mg
158 of solution was weighed in an aluminum pan, sealed hermetically, cooled to -40°C and held for 15
159 minutes and warmed to 10°C at 10, 5 and 0.5°C/min.

160 In another set of studies, about 20 mg of the aqueous solutions were weighed into an aluminum
161 pan, sealed hermetically, and cooled from room temperature to -60°C at 1°C/min, held
162 isothermally for 10 min, and heated at 1°C/min to room temperature, under a stream of nitrogen.
163 Annealing/temperature cycling was performed to achieve maximum solute and ice crystallization.
164 Samples were annealed at -20°C for 2 to 16 hours above Tg' of the system during warming. The
165 solutions were cooled to -60°C and rewarmed, the Tg', heat capacity associated with Tg' (ΔCp)
166 and the enthalpy of ice and solute melting endotherms in the final warming curve were recorded.

167 **2.3. *Synchrotron XRD (Transmission Mode)***

168 Phase transformations during freezing and warming were also characterized at the synchrotron X-
169 ray beamline 17-BM-B (sector 17; Advanced Photon Source, Argonne National Laboratory, IL,
170 USA). A monochromatic X-ray beam ($\lambda=0.45452$ Å, beam size 300 μm x 300 μm) and a two-
171 dimensional (2D) area detector (XRD-1621, Perkin Elmer) were used. More details with respect
172 to the experimental setup can be found in our earlier publication (Bhatnagar et al., 2020).

173 The aqueous solutions were placed in a custom-made copper sample holder with a Kapton®
174 window, polyether ether ketone (PEEK) base and a thermocouple. A T-thermocouple (Omega)
175 was used to record the real-time temperature using a temperature input device (NI USB-TC01,
176 National Instruments, TX). Freezing and warming of 100 μL of sample placed in the V-shaped
177 copper sample holder was carried out with the aid of Cryostream 700 plus (Oxford Cryosystems
178 Ltd, Oxford, UK) adjusted 3 to 5 cm above the sample holder. The temperature difference between
179 the cryostream and sample holder was determined by cooling an aqueous sodium chloride (23%

180 w/w) solution and determining the sodium chloride - water eutectic temperature. Background
181 signal was collected by exposing the sample holder without any solution. The 2D X-ray patterns
182 collected were converted to 1D 2θ scans using GSAS-II software (Edgewall Software) (Toby and
183 Von Dreele, 2013). The crystalline phases were identified, and the integrated peak intensities were
184 determined using commercial software (JADE 2010, Material Data, Inc.).

185 **2.4. *Size Exclusion High Performance Liquid Chromatography (SE-HPLC)***

186 Protein aggregation in formulations was monitored by determining the % monomer and % high
187 molecular weight species (HMWS) using SE-HPLC. An ACQUITY UPLC Protein BEH 200 SEC
188 column was used on an ACQUITY UPLC H class system with UV detection (Waters Corporation,
189 Milford, MA). The mobile phase solution contained 0.2 M Sodium Phosphate at pH 6.8. Injection
190 volume for each sample was 20 μ L and the flow rate was 0.5 mL/min. Absorbance of the eluent
191 at 220 nm and 280 nm was measured and chromatograms were analyzed using Empower® 3
192 software (Waters Corporation, Milford, MA).

193 **2.5. *Freeze-thaw***

194 Freeze-thawing was carried out in a benchtop freeze-dryer (VirTis AdVantage, Gardiner, NY).
195 Each formulation was filled (3 mL) in 10 mL glass vials (DWK Wheaton, IL). For unannealed
196 samples, the vials were first cooled from 25°C to 5°C, held for 30 min, and further cooled to -
197 40°C and held for 30 minutes. The frozen samples were thawed back to 20°C with an isothermal
198 hold step at 5°C for 30 minutes. Both cooling and thawing rates were 1°C/min. After thawing the
199 vials were swirled. The process of freeze-thawing was repeated 5 times. Similar protocol was used
200 for annealed samples with an additional annealing (isothermal hold) step at -20°C for 2 hours.

201

202 **3. RESULTS AND DISCUSSION**

203 ***3.1. Mannitol-sucrose systems***

204 Thermal characterization of different ratios of mannitol to sugar were performed using DSC. The
205 solutions were cooled from RT to -40 °C and then heated to RT at cooling and heating rates of
206 either 10 or 5 °C/min. A higher ramp rate was chosen to screen the thermal behavior of with
207 different mannitol to sugar ratios with the goal of identifying compositions in which mannitol
208 crystallization was observed during cooling. However, only the final heating curves are shown
209 (Figure 1 and 3). At M:S ratios of 1:1, 1:2 and 1:4, there was no evidence of mannitol
210 crystallization, both during cooling (not shown) and heating (Figure 1, panels A (10 °C/min) and
211 C (5 °C/min)). At a M:S ratio of 2:1, an exotherm was observed during heating, attributable to
212 mannitol crystallization (Figures 1 A and C). The DSC curve of this composition has been
213 expanded in panels B and D. The system was characterized by two glass transition events, T_g''
214 (lower temperature transition) at ~-32 °C and T_g' at ~ -27 °C and these seemed to be unaffected
215 by the cooling rate. However, at the lower cooling rate of 5 °C/min, there was an increase in the
216 fraction of mannitol crystallizing from solution (enthalpy of exotherm at ~ 10 °C; panels B and D).
217 When the cooling rate was decreased to 0.5° C/min, there was evidence of mannitol crystallization
218 during cooling (exotherm at ~-23 °C; Figure 2A). The inset is an expanded view. When the
219 solution was heated, again a crystallization exotherm was observed at ~ -25 °C. Thus,
220 crystallization of mannitol was not complete during cooling. This amorphous fraction crystallized
221 during heating, immediately above the T_g' .

222

223 ***3.2. Mannitol-trehalose systems***

224 Qualitatively similar results were obtained in M:T systems with different ratios (Figure 3, panels
225 A and C). Though this system also exhibited two glass transition events (T_g' and T_g''), the cooling

226 rate influenced their values. However, this was not investigated further. The enthalpy of mannitol
227 crystallization was much higher in presence of trehalose (Figure 3 B and D). It is known that
228 trehalose facilitates mannitol crystallization (Jena et al., 2016). The influence of trehalose was
229 further evident at a slower cooling rate of 0.5 °C/min (data not shown). There was pronounced but
230 incomplete crystallization of mannitol during cooling. However, the amorphous fraction
231 crystallized during heating (Figure 4). Thus, the crystallization behavior of mannitol was similar
232 in the presence of the two sugars, sucrose and trehalose. When the cooling rate was further
233 decreased to 0.1 °C/min, mannitol appeared to crystallize completely during cooling
234 (supplementary information; Figure S1). An exotherm, attributable to mannitol crystallization, was
235 not observed during heating and the system was characterized by a single glass transition event at
236 ~ -32 °C (Figure 5 B).

237 To evaluate in greater detail the crystallization behavior of mannitol during cooling, the mannitol:
238 trehalose ratio was increased (3:1). At a cooling rate of 0.1°C/min, ice crystallization occurred
239 earlier (exotherm at ~ -5 °C) and was followed by a second crystallization exotherm at ~ -16 °C
240 with an enthalpy of crystallization of ~9 J/g (supplementary information; Figure S2). Interestingly,
241 when this sample was heated from -40 °C to 10 °C (at 0.1 °C/min), the Tg' as well as the mannitol
242 crystallization exotherm were not seen (data not shown). This suggests that the crystallization
243 exotherm post ice crystallization during cooling can be attributed to mannitol crystallization. The
244 high enthalpy value (~9 J/g), coupled with the absence of crystallization exotherm during heating,
245 suggests complete mannitol crystallization during cooling. The absence of glass transition during
246 heating also supports this contention.

247 Synchrotron XRD experiments performed during cooling from room temperature to -45°C
248 followed by heating the frozen solution back to room temperature at 1°C/min helped in further

249 understanding of the mannitol-trehalose 3:1 (5% w/v) system. During cooling, ice peaks first
250 appeared at ~ -9°C followed by appearance of mannitol hemihydrate peaks at ~ -18°C (Figure 7
251 A). Further cooling to -45°C resulted in a slight increase in the hemihydrate and ice peak
252 intensities. It was evident from the shape of the peaks that ice crystallization was substantially
253 incomplete, indicating that a large fraction of the solute was in the freeze-concentrate along with
254 unfrozen water. In addition, the heterogeneity of the freeze-concentrate was evident from the two
255 glass transitions observed in the DSC. During heating, until ~ -23°C, the hemihydrate and ice peaks
256 did not reveal any change in peak intensity. Further heating resulted in (i) increase in the
257 hemihydrate as well as ice peak intensities, and (ii) transition of the hemihydrate to δ -form of
258 mannitol prior to eutectic melting at ~ 0°C. A pronounced and sharp increase in mannitol peak
259 intensities was observed around T_g' . Thus, the pronounced crystallization propensity of mannitol
260 at $T > T_g'$, observed earlier in the DSC (Figures 1 and 3; panels B and D) was supported by the
261 XRD results.

262 The propensity of an excipient to crystallize during thawing can have implications on protein
263 stability. The effects would be exacerbated if a system undergoes multiple freeze-thaw cycles.
264 Since proteins are stored frozen, often for prolonged time periods, freeze-thaw studies provide an
265 avenue to understand the impact of long term frozen storage. These results have some important
266 practical implications. Desai et al showed in a glycine mAb formation, protein aggregation
267 increased when the thawing rate was decreased (Desai, 2017). They attributed aggregation during
268 thawing to the crystallization of glycine. The perturbations at the ice-liquid interface brought about
269 by the crystallization of the unfrozen water associated with solute could be a major destabilizing
270 factor. Thus, the existence of amorphous solute in the frozen state, which can then recrystallize
271 during heating can be a source of protein instability. It is instructive to note that during slow

272 thawing, it is not the solute crystallization per se, but the formation of these “new” ice interfaces
273 (at $T > T_g'$) that is the major destabilizing factor (Figure 7B).

274 **3.3. *Mannitol-trehalose (3:1) systems – effect of isothermal hold***

275 The next objective was to determine the effect of holding at -20 °C for different time periods on
276 the phase behavior of excipient mixtures. Mannitol and trehalose individually are known to exhibit
277 two characteristic glass transition temperatures. The glass transition temperatures of mannitol (5%
278 w/w) were ~ -32 (T_g'') and ~ -25°C (T_g') and of trehalose were ~ -45°C (T_g'') and ~ -31°C
279 (T_g') (Pyne et al., 2002). The T_g'' value of -31°C for the mannitol-trehalose (3:1) is close to the
280 T_g'' values of mannitol (-32°C). However, the T_g' value (-32°C) of the mixture was closer to the
281 T_g' of trehalose (Figure 6A). The two glass transitions likely reflect the existence of two slightly
282 different compositions in the freeze concentrate. The composition with the lower glass transition
283 (T_g'') is expected to contain a higher amount of unfrozen water and this can be thought of as a
284 “water-rich phase”. The composition with the higher glass transition (T_g') is likely the maximally
285 freeze-concentrated phase. The ΔC_p value can be an approximate measure of the “amount” of
286 amorphous phase. The ΔC_p values associated with T_g'' and T_g' were 0.19 and 0.09 J/g°C
287 respectively (Table 1). Based on this, the composition characterized by T_g'' would constitute the
288 larger amorphous fraction.

289 After the cooling rate was optimized in section 3.2, the effect of annealing during cooling, on the
290 crystallization behavior of mannitol was investigated. The solutions were cooled to -20° C at 0.5
291 °C/min and held for up to 16 hours. They were then further cooled to -60°C and then heated back
292 to RT. In the absence of isothermal hold, T_g'' and T_g' were observed at ~ -41 and -32 °C
293 respectively (Figure 6A). When held for ≥ 2 hours at -20°C, the T_g'' disappeared while the T_g'
294 remained unaffected (Figure 6B). Thus, holding at -20 °C even for only 2 hours seems to cause
295 complete crystallization of the composition with the higher water content. There was also a

296 pronounced reduction in ΔC_p associated with T_g' suggesting substantial crystallization of this
297 composition (Figure 6B). The holding time was progressively increased up to 16 hours. The T_g'
298 remained unaffected confirming that this was the maximally freeze-concentrated system of
299 constant composition (confirmed in the synchrotron XRD studies in the next section). There
300 appeared to be a small decrease in the magnitude of ΔC_p at the longer annealing times. However,
301 these results should be viewed with caution in light of the low ΔC_p values. Finally, the enthalpy
302 of fusion (mannitol-ice eutectic + ice melting) also provided evidence of amorphous phase
303 crystallization due to the isothermal hold at -20 °C. Holding for 2 hours, caused an appreciable
304 increase in the enthalpy value (Table 1). This could be a consequence of the crystallization of
305 mannitol and the associated unfrozen water. Holding for a longer time period did not have any
306 noticeable effect on the observed enthalpy value. This result is not surprising in light of the small
307 change in ΔC_p (T_g') at holding times > 2 hours (Table 1). Annealing the samples at -37°C - a
308 temperature above T_g'' (- 41°C) but below T_g' (-32°C) for 2 hours, resulted in disappearance of
309 the T_g'' . On reheating, a single glass transition was observed at -34°C followed by an exotherm
310 attributable to mannitol crystallization. Thus, when annealed at a temperature below T_g' , mannitol
311 was retained amorphous (supplementary information; Figure S3).

312 The effect of annealing on the crystallization behavior of mannitol and ice could be discerned from
313 synchrotron XRD experiments performed during cooling (Figure 8A). Ice crystallization was the
314 first event observed (~ -10°C) followed by the appearance of β -mannitol peaks at -12°C. During
315 the isothermal hold at -12°C, there was a pronounced increase in the intensities of both mannitol
316 and ice peaks. This was in line with the earlier report of Mehta et al that MHH formation was
317 completely prevented when crystallization occurred between -10 and -15°C (Mehta et al., 2013).
318 Once β -mannitol and ice peaks formed during annealing at -12°C, the peak intensities increased,

319 both during annealing and further cooling until -15°C (Figure 8A). On further cooling to -40°C,
320 there was negligible change in the peak intensities.

321 On heating the frozen system from -45°C to -2°C, there was no increase in ice and mannitol peak
322 intensities up to ~ - 5°C. There was then a progressive decrease in the peak intensities until they
323 disappeared at ~ 1°C (Figure 8B). Thus, the behavior of the annealed system during heating was
324 very different from that of the unannealed solutions (compared Figures 7B and 8B).

325 The XRD results revealed that annealing during cooling enabled us to: (i) promote selective
326 crystallization of the anhydrous form of mannitol, and (ii) maximize ice crystallization during
327 cooling and thereby minimize the residual unfrozen water crystallization during heating (post Tg').

328 However, there is one potential challenge. It is well known that mannitol crystallization can
329 promote trehalose crystallization (Sundaramurthi and Suryanarayanan, 2010). The crystallization
330 of trehalose would be highly undesirable since it could compromise its cryoprotectant function. In
331 order to minimize the risk of trehalose crystallization, its concentration was low (1.25%).

332 Moreover, in spite of the high sensitivity of the technique, there was no evidence of trehalose
333 crystallization (Figure 8). In frozen aqueous systems, trehalose crystallizes as a dihydrate with
334 characteristic peaks at 8.8 and 12.6°2θ (Sundaramurthi et al., 2010). These peaks were absent in
335 the frozen solutions (Figure 8). DSC provided additional evidence of the potential for trehalose to
336 be retained in the amorphous state. Even when the annealing time was increased up to 24 hours,
337 the Tg' was invariant (- 31°C) suggesting the retention of a freeze concentrate of constant
338 composition.

339 Thus, with the judicious selection of the concentrations of trehalose and mannitol, while substantial
340 crystallization of mannitol can be accomplished the trehalose is retained amorphous. Thus, the risk

341 of trehalose-crystallization induced loss in cryoprotection would be minimized while causing
342 substantial (if not complete) crystallization of mannitol in the desired anhydrous state
343 Thus, annealing during cooling enabled us to: (i) promote the selective crystallization of the
344 anhydrous form of mannitol, and (ii) obtain a single maximally freeze-concentrated phase of
345 constant composition (T_g').

346 **3.4. *Mannitol-sucrose (3:1) systems – effect of isothermal hold***

347 The behavior of mannitol-sucrose (3:1) systems was substantially similar to that of mannitol-
348 trehalose (3:1). While the DSC curves are not shown, the results are summarized in Table 2. The
349 T_g'' and the T_g' values were virtually identical for the unannealed mannitol-trehalose and
350 mannitol-sucrose systems (Tables 1 and 2). The one notable difference was the ΔC_p at T_g'' which
351 was much less (0.08 J/g°C) for the sucrose containing systems. When this “population” was
352 removed by annealing, presumably by crystallization of mannitol and the associated unfrozen
353 water, the attendant increase in the enthalpy of fusion (overlapping of mannitol-ice eutectic and
354 ice melting) was small (from 328 to 333 J/g; Table 2).

355 **3.5. *HSA aggregation: Effect of processing (annealed versus unannealed) and composition***

356 Using HSA (1 mg/mL) as a model protein, in selected mannitol-sucrose and mannitol-trehalose
357 buffered solutions, we evaluated the impact of processing on protein aggregation. Selected
358 compositions were also subjected to DSC, at a cooling rate of 1°C/ min, with and without an
359 isothermal hold step. HSA, at a concentration of 1 mg/mL, had no significant impact on mannitol
360 phase behavior (data not shown). Buffered protein solutions in mannitol, sucrose, or trehalose
361 alone and in mannitol-sugar (1:1 and 3:1) mixtures were subjected to multiple freezing and
362 thawing cycles (5 F/T). The 5 freeze-thaw cycles were conducted at a ramp rate of 1°C/min. One
363 set of samples were frozen with an annealing step at -20°C for 2 hours during cooling, while the

364 other set did not include annealing. The protein stability before and after freezing and thawing was
365 evaluated by SE-HPLC.

366 We will first look at the effect of freeze-thaw stress on unannealed HSA formulations that
367 contained either mannitol, sucrose or trehalose individually. Generally, increased protein
368 aggregation after multiple F/T cycles is not uncommon due to the stresses proteins encounter
369 throughout freezing and thawing. All the formulations that were subjected to 5 F/T cycles showed
370 an increase in high molecular weight species (HMWS) compared to their respective controls
371 (Figure 9). The most pronounced increases in %HMWS ($\geq 1.5\%$) were observed in the freeze-
372 thawed formulations containing mannitol or trehalose. In the former case, this is attributed to phase
373 separation brought about by crystallization of mannitol, and the consequent lack of cryoprotection.
374 It is important to note that there was pronounced mannitol crystallization during thawing (Figure
375 7b) which explains aggregation in mannitol alone formulations. While trehalose remained
376 amorphous, HSA aggregation was observed. We expected the %HMWS to be lower in this
377 formulation since trehalose is a commonly used cryoprotectant. Additional studies would be
378 needed to understand this result.

379 There was a favorable effect of annealing in the HSA formulation that contained mannitol. In case
380 of mannitol, there are two possible stabilization mechanisms. Substantial crystallization of
381 mannitol during annealing, resulting in a homogenous freeze-concentrate may have facilitated
382 protein stabilization. Secondly, there was no evidence of mannitol crystallization during thawing
383 (Figure 8b). As a result, there was no generation of “new” ice interfaces during thawing – hence
384 the potential for reduced protein aggregation. While the effect of annealing was less pronounced
385 in the presence of sucrose, the process resulted in a single T_g' again indicating a homogenous
386 freeze-concentrate while monomer was substantially retained. While annealing also resulted in a

387 single Tg' in the trehalose system, there was no reduction in % HMWS compared to the
388 unannealed formulation.

389 Next, the effect of mannitol-sucrose combination (1:1) was compared with the individual solutes.
390 The %HMWS after 5 freeze-thaw cycles in mannitol-sucrose combinations was much lower than
391 in mannitol or sucrose alone for both annealed and unannealed samples. This composition appears
392 to be better than all the other systems investigated. Similarly, the mannitol-trehalose combination
393 (1:1) performed better than the individual solutes and annealing resulted in pronounced
394 stabilization.

395 Increasing the mannitol concentration, either with sucrose or with trehalose (3:1) did not have an
396 evident impact on HSA aggregation compared to respective 1:1 compositions. The stabilizing
397 effect of sucrose was readily evident.. The 3:1 mannitol-sugar combinations also had less
398 aggregation than respective formulations composed of mannitol, sucrose, or trehalose alone.
399 However, annealing did not appear to have any additional stabilizing effect. This result is not
400 surprising because mannitol is present at a much higher concentration than the sugar (3:1), it
401 crystallized readily during cooling (Table 1). Thus, the annealing step is not expected to bring
402 about additional mannitol crystallization and the consequent stabilization.

403 Micro-flow imaging (MFI) was used to characterize sub-visible particles. However, no
404 meaningful trends were observed. The subvisible particles counts for all solutions before and
405 after freeze-thaw were low and were less than 6,000 particles >10 micron and less than 600
406 particles > 25 micron (supplementary information; Table S1). In other words, the systems met
407 the USP specifications (USP 787/788).

408 As we compare the two sugars, over a range of compositions as well as the effect of the annealing
409 step, the superiority of sucrose is consistently evident. The underlying mechanism of

410 cryoprotection was outside the scope of this work. Interestingly, the mannitol-sugar combination
411 with annealing performed better or equivalent to the sugar alone formulations in terms of protein
412 stabilization. Although limited to a single protein (HSA), the most pronounced stabilization effect
413 following annealing was observed at a 1:1 mannitol-sugar ratio. This supports our hypothesis that
414 inclusion of mannitol along with sugar and causing complete mannitol crystallization during
415 freezing can generate a homogeneous matrix where protein stability can be maintained or even
416 improved.

417 **4. Conclusion**

418

419 Freezing and thawing are critical unit operations in biotherapeutic manufacturing. A lack of control
420 in these steps, and specifically, fast freezing and slow thawing appeared to facilitate protein
421 aggregation. The addition of mannitol and facilitating its crystallization through annealing enabled
422 us to obtain a homogenous freeze-concentrate with a single glass transition (T_g'). Thus, annealing
423 during cooling enabled us: (i) promote the selective crystallization of the anhydrous form of
424 mannitol, and (ii) obtain a single maximally freeze-concentrated phase of constant composition
425 (T_g'). Including an annealing step during freezing can be a practical approach to maximize
426 excipient, as well as associated unfrozen water crystallization, early in the freezing process. This
427 approach can minimize, if not eliminate, the need for precise control of the freezing and thawing
428 rates. This protocol can also be applied for drug substance storage, wherein the storage temperature
429 $< T_g'$.

430 **Declaration of Competing Interest**

431 The authors declare that they have no known competing financial interests or personal
432 relationships that could have appeared to influence the work reported in this paper.

433 **Acknowledgements**

434 We acknowledge funding from the Kildsig Center for Pharmaceutical Processing Research and
435 the support of the William and Mildred Peters Endowment Fund. Use of the Advanced Photon
436 Source was supported by U.S. Department of Energy, Office of Science, Office of Basic Energy
437 Science, under Contract No. DE-AC02-06CH11357. We thank Dr. Wenqian Xu and Dr. Andrey
438 Yakovenko for their help during the beamline experiments.

439

440

441

442 **References**

443 Arsiccio, A., Pisano, R., 2020. The Ice-Water Interface and Protein Stability: A Review. *J Pharm*
444 *Sci.*<https://doi.org/10.1016/j.xphs.2020.03.022>

445 Authelin, J.R., Rodrigues, M.A., Tchessalov, S., Singh, S.K., McCoy, T., Wang, S., Shalaev, E., 2020.
446 Freezing of Biologicals Revisited: Scale, Stability, Excipients, and Degradation Stresses. *J Pharm Sci* 109,
447 44-61.[10.1016/j.xphs.2019.10.062](https://doi.org/10.1016/j.xphs.2019.10.062)

448 Bhatnagar, B.S., Bogner, R.H., Pikal, M.J., 2007. Protein stability during freezing: separation of stresses
449 and mechanisms of protein stabilization. *Pharm Dev Technol* 12, 505-
450 523.<https://doi.org/10.1080/10837450701481157>

451 Bhatnagar, B.S., Sonje, J., Shalaev, E., Martin, S.W., Teagarden, D.L., Suryanarayanan, R., 2020. A refined
452 phase diagram of the tert-butanol–water system and implications on lyophilization process optimization
453 of pharmaceuticals. *Phys Chem Chem Phys*

454 Carpenter, J.F., Pikal, M.J., Chang, B.S., Randolph, T.W., 1997. Rational design of stable lyophilized
455 protein formulations: some practical advice. *Pharm Res* 14, 969

456 Chang, L.L., Pikal, M.J., 2009. Mechanisms of protein stabilization in the solid state. *J Pharm Sci* 98, 2886-
457 2908

458 Connolly, B.D., Le, L., Patapoff, T.W., Cromwell, M.E.M., Moore, J.M.R., Lam, P., 2015. Protein
459 Aggregation in Frozen Trehalose Formulations: Effects of Composition, Cooling Rate, and Storage
460 Temperature. *J Pharm Sci* 104, 4170-4184.[10.1002/jps.24646](https://doi.org/10.1002/jps.24646)

461 Desai, K.G., W. Aaron Pruett, Peter J. Martin, James D. Colandene, and Douglas P. Nesta, 2017. Impact of
462 manufacturing-scale freeze-thaw conditions on a mAb solution. *BioPharm Int* 30 no. 2, 30-36

463 Hancock, B.C., Zografi, G., 1997. Characteristics and significance of the amorphous state in
464 pharmaceutical systems. *Journal of pharmaceutical sciences* 86, 1-12

465 Jena, S., Horn, J., Suryanarayanan, R., Friess, W., Aksan, A., 2017. Effects of excipient interactions on the
466 state of the freeze-concentrate and protein stability. *Pharm Res* 34, 462-478

467 Jena, S., Suryanarayanan, R., Aksan, A., 2016. Mutual influence of mannitol and trehalose on
468 crystallization behavior in frozen solutions. *Pharm Res* 33, 1413-1425

469 Johnson, R.E., Kirchhoff, C.F., Gaud, H.T., 2002. Mannitol-sucrose mixtures--versatile formulations for
470 protein lyophilization. *J Pharm Sci* 91, 914-922.10.1002/jps.10094

471 Kim, A.I., Akers, M.J., Nail, S.L., 1998. The physical state of mannitol after freeze-drying: effects of
472 mannitol concentration, freezing rate, and a noncrystallizing cosolute. *J Pharm Sci* 87, 931-935

473 Kolhe, P., Badkar, A., 2011. Protein and solute distribution in drug substance containers during frozen
474 storage and post-thawing: A tool to understand and define freezing–thawing parameters in
475 biotechnology process development. *Biotechnology progress* 27, 494-504

476 Mehta, M., Bhardwaj, S.P., Suryanarayanan, R., 2013. Controlling the physical form of mannitol in
477 freeze-dried systems. *Eur J Pharm Biopharm* 85, 207-213

478 Piedmonte, D.M., Summers, C., McAuley, A., Karamujic, L., Ratnaswamy, G., 2007. Sorbitol crystallization
479 can lead to protein aggregation in frozen protein formulations. *Pharm Res* 24, 136-146.10.1007/s11095-
480 006-9131-1

481 Pyne, A., Surana, R., Suryanarayanan, R., 2002. Crystallization of mannitol below T_g' during freeze-drying
482 in binary and ternary aqueous systems. *Pharm Res* 19, 901-908

483 Rathore, N., Rajan, R.S., 2008. Current perspectives on stability of protein drug products during
484 formulation, fill and finish operations. *Biotechnology progress* 24, 504-514

485 Searles, J.A., Carpenter, J.F., Randolph, T.W., 2001. Annealing to optimize the primary drying rate,
486 reduce freezing-induced drying rate heterogeneity, and determine T_g' in pharmaceutical lyophilization.
487 *Journal of pharmaceutical sciences* 90, 872-887

488 Singh, S., Kolhe, P., Wang, W., Nema, S., 2009. Large Scale Freezing of Biologics, A Practitioner's Review,
489 Part One: Fundamental Aspects. *Bioprocess Int.* 7, 32-44

490 Sundaramurthi, P., Patapoff, T.W., Suryanarayanan, R., 2010. Crystallization of trehalose in frozen
491 solutions and its phase behavior during drying. *Pharm Res* 27, 2374-2383

492 Sundaramurthi, P., Suryanarayanan, R., 2010. Trehalose crystallization during freeze-drying: implications
493 on lyoprotection. *J Phys Chem Lett* 1, 510-514

494 Toby, B.H., Von Dreele, R.B., 2013. GSAS-II: the genesis of a modern open-source all purpose
495 crystallography software package. *J. Appl. Crystallogr* 46, 544-549

496 Wang, W., 2005. Protein aggregation and its inhibition in biopharmaceutics. *Int J Pharm* 289, 1-
497 30.10.1016/j.ijpharm.2004.11.014

498

499

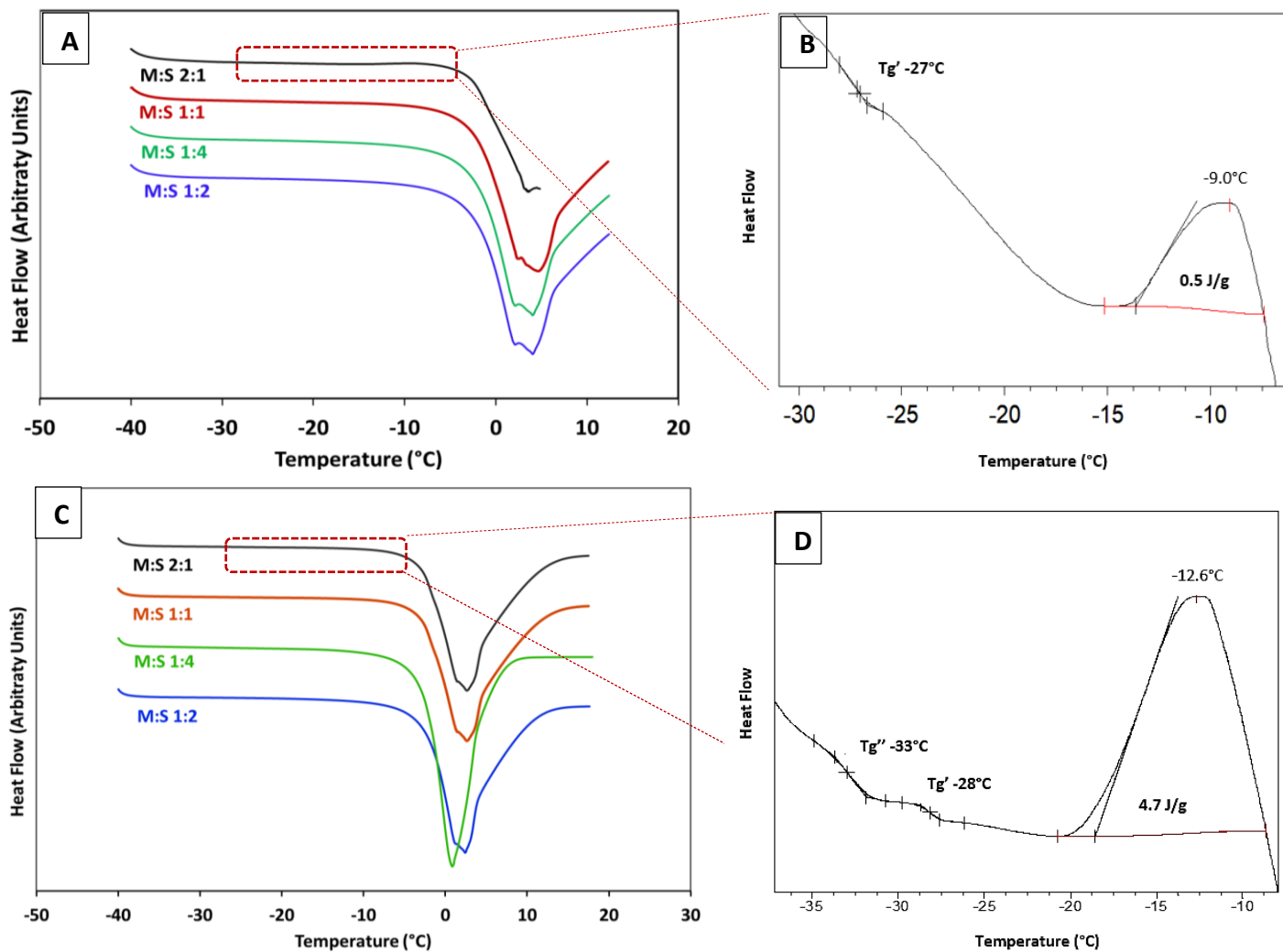
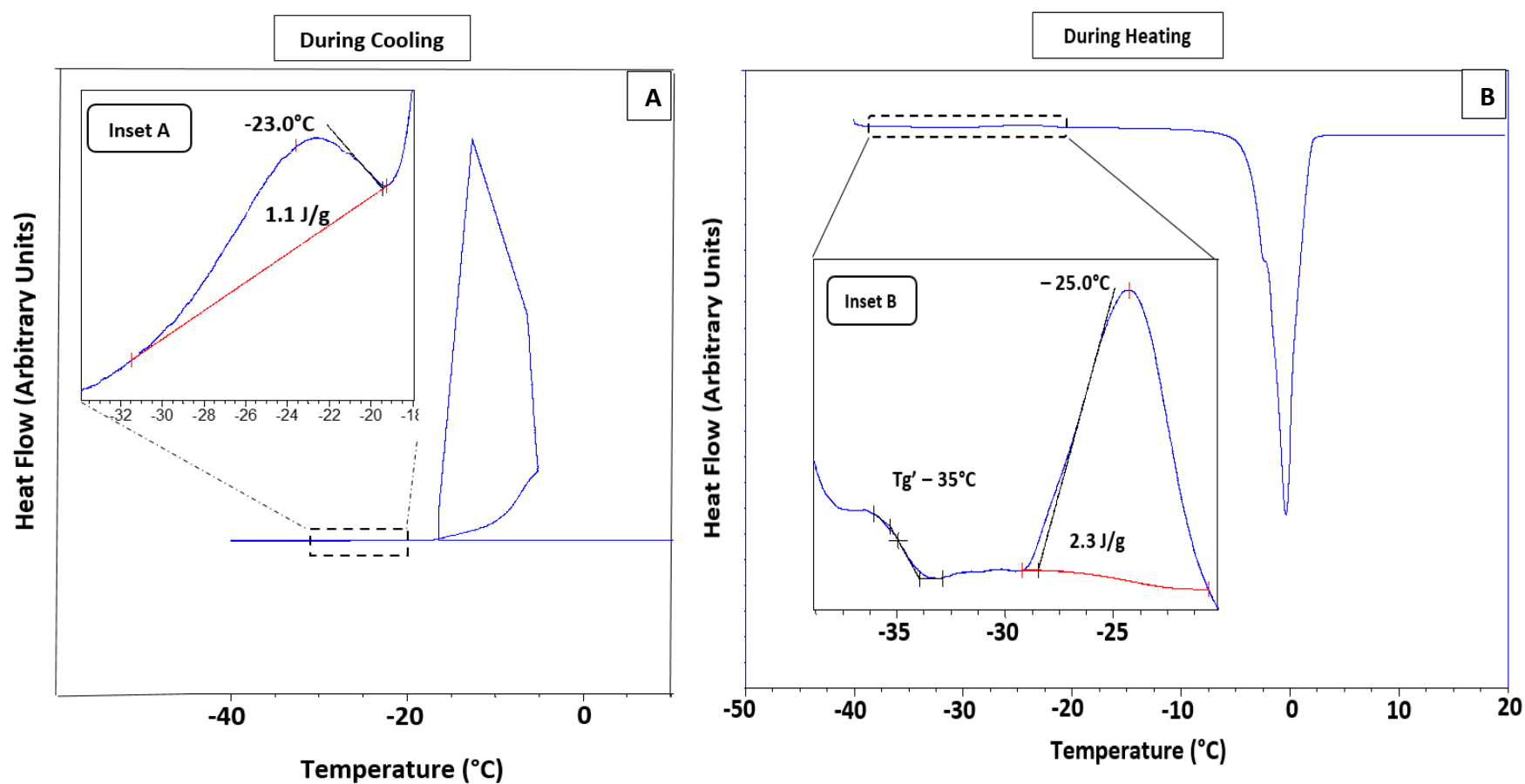


Figure 1. Overlaid DSC heating curves for four different mannitol-sucrose ratios (1:4, 1:2, 1:1 and 2:1) with a solute concentration of 5% w/v. Panel A. The solutions were initially cooled from room temperature to -40°C at 10°C/minute held for 5 minutes and heated to 15°C at 10°C/minute. Only the heating curves are shown. Panel B. Shows a magnified region with T_g' and crystallization exotherm for mannitol-sucrose 2:1 solution from panel A. Panel C. The solutions were initially cooled from room temperature to -40°C at 5°C/minute held for 5 minutes and heated to 15°C at 5°C/minute. Only the heating curves are shown. Panel D. Shows a magnified region with T_g'' and crystallization exotherm for mannitol-sucrose 2:1 solution from panel C.



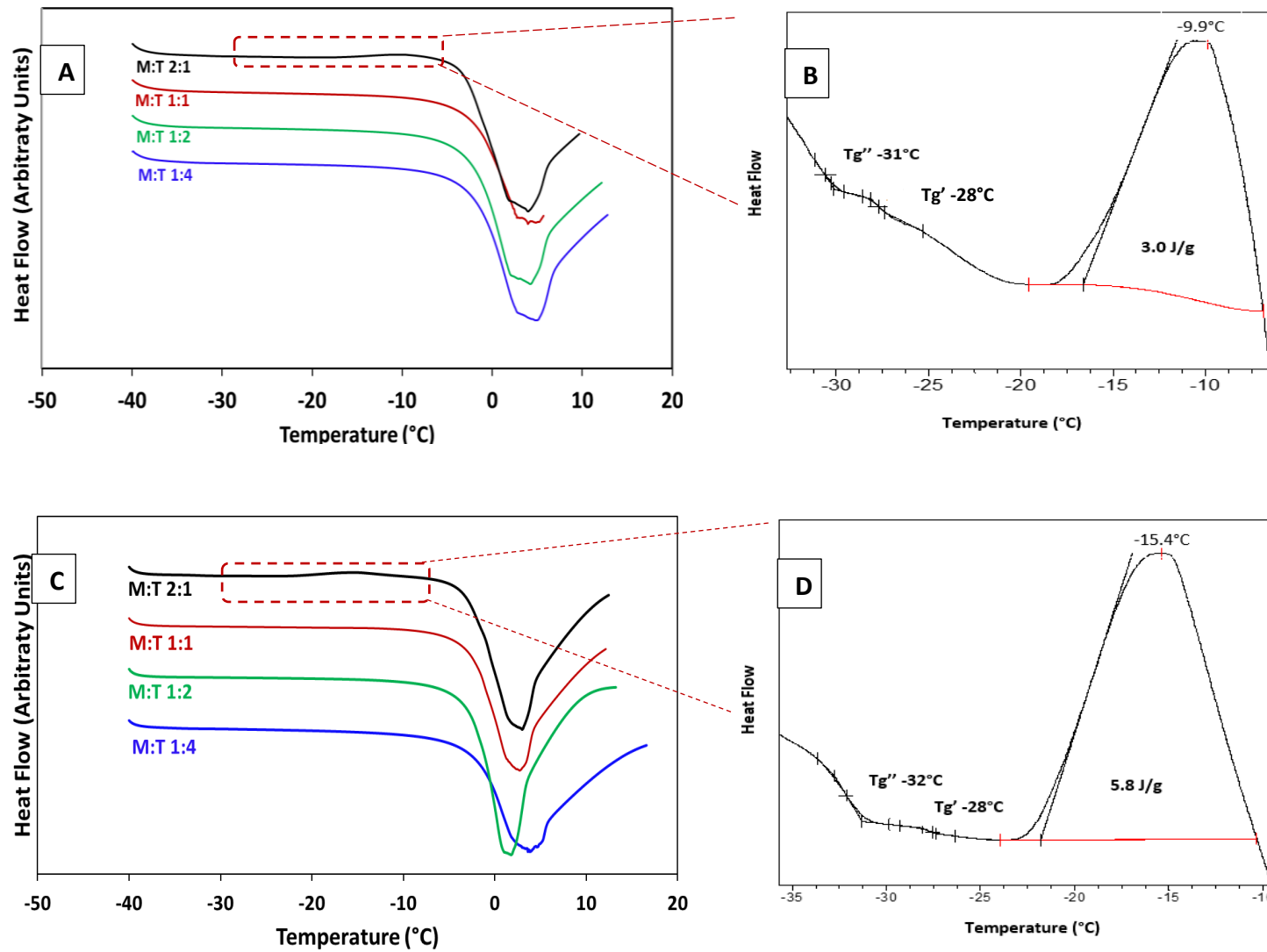
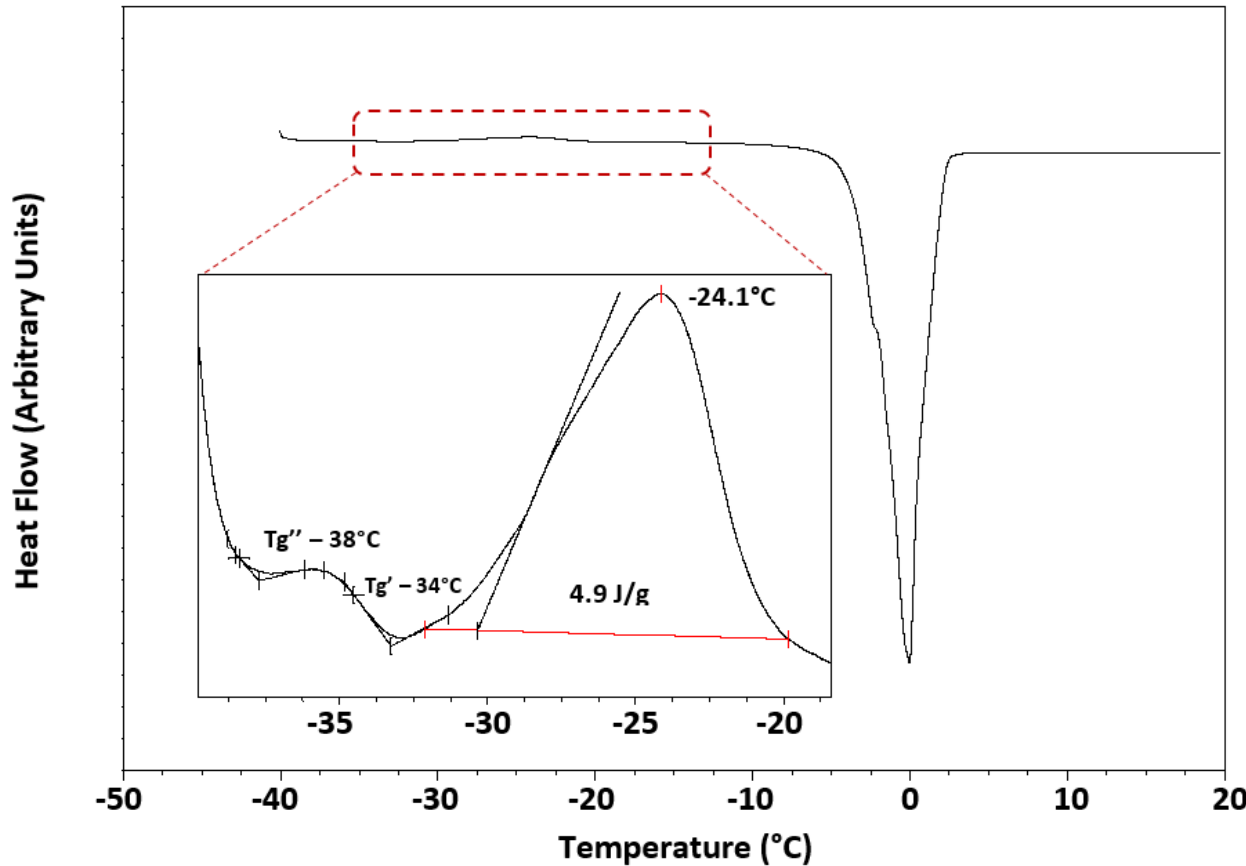


Figure 3. Overlaid DSC heating curves for four different mannitol-trehalose ratios (1:4, 1:2, 1:1 and 2:1) with a solute concentration of 5% w/v. Panel A. The solutions were initially cooled from room temperature to -40°C at 10°C/minute held for 5 minutes and heated to 15°C at 10°C/minute. Only the heating curves are shown. Panel B. Shows a magnified region with T_g' and crystallization exotherm for mannitol-trehalose 2:1 solution from panel A. Panel C. The solutions were initially cooled from room temperature to -40°C at 5°C/minute held for 5 minutes and heated to 15°C at 5°C/minute. Only the heating curves are shown. Panel D. Shows a magnified region with T_g' and crystallization exotherm for mannitol-trehalose 2:1 solution from panel C.



573

574 **Figure 4.** Mannitol-trehalose 2:1 composition. DSC heating curve from -40°C to 25°C at $0.5^\circ\text{C}/\text{min}$. The inset shows glass transition and
575 crystallization exotherm from -40 to -20°C . The sample was cooled from room temperature to -40°C at $0.5^\circ\text{C}/\text{min}$ (cooling curve not shown).

576

577

578

579

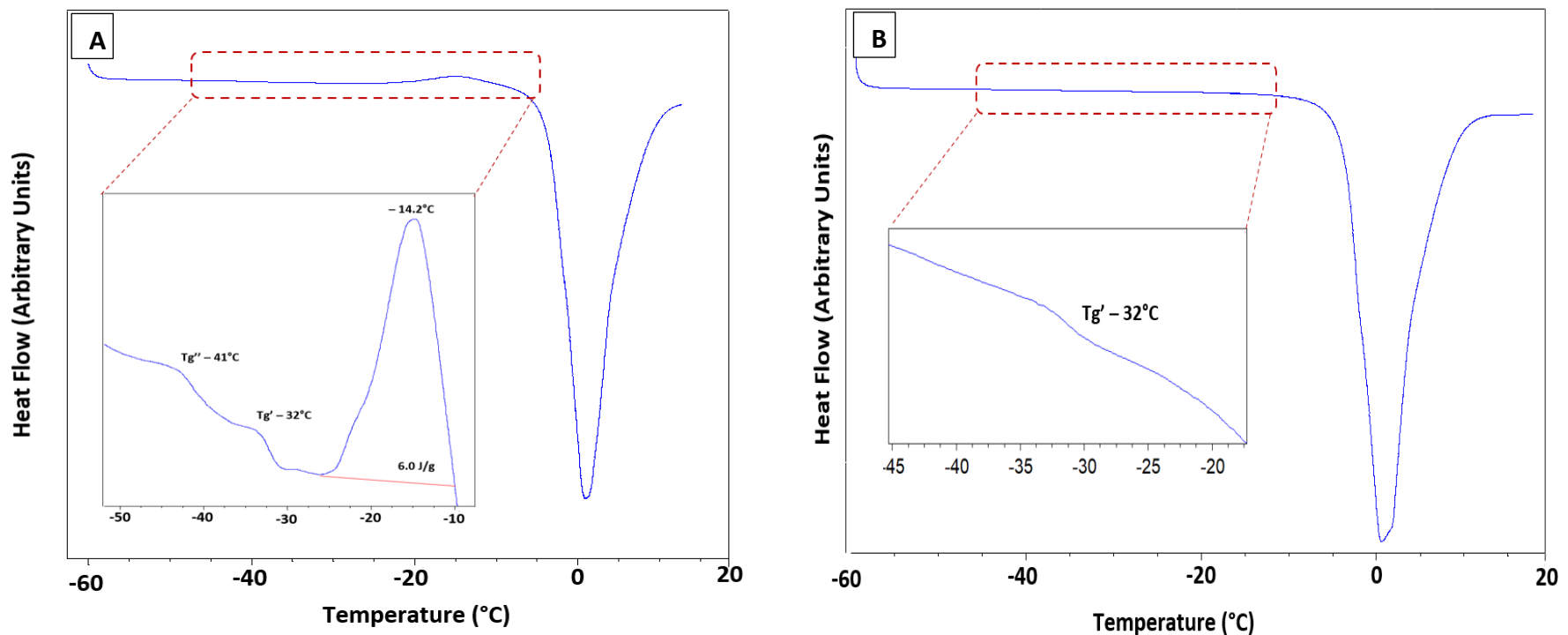


Figure 5. DSC heating curves for mannitol-trehalose 3:1 (A) sample was cooled to -20°C at $0.5^{\circ}\text{C}/\text{min}$ held for 2 minutes and further cooled to -60°C at $5^{\circ}\text{C}/\text{min}$. The frozen sample was heated to 20°C at $5^{\circ}\text{C}/\text{min}$. Only the heating curve is shown in the figure. (B) sample was cooled to -20°C at $0.5^{\circ}\text{C}/\text{min}$ held for 2 hours and further cooled to -60°C at $5^{\circ}\text{C}/\text{min}$. The frozen sample was heated to 20°C at $5^{\circ}\text{C}/\text{min}$. The heating curve in the figure shows the presence of only glass transition event.

Table 1. Mannitol-trehalose (3:1) – DSC data for isothermal hold (-20°C) experiments

Formulation	Annealing time at -20°C during cooling (hours)	Tg”		Tg'	Tc		ΔH (J/g) at Tm (Ice and mannitol-ice eutectic melting)
		Temperature (°C)	ΔC_p (J/g°C)	Temperature (°C)	Temperature (°C)	ΔH (J/g)	
Mannitol:trehalose 3:1	No annealing	-41.5 ± 0.1	0.19 ± 0.0	-32 ± 0.1	-21	6.28 ± 0.2	323.0 ± 2.0
	2			-31 ± 0.2			336.7 ± 2.0
	4			-32 ± 0.0			339 ± 2.0
	8			-32 ± 0.0			336.1 ± 3.2
	16			-31 ± 0.0			333.0 ± 0.4

605 **Variability in the results are reported in terms of standard deviation (n=3)**

606 **Table 2.** Mannitol-sucrose (3:1) – DSC data for isothermal hold (-20°C) experiments

Formulation	Annealing time at -20°C during cooling (hours)	Tg”		Tg'	Tc		ΔH (J/g) at Tm (Ice and mannitol-ice eutectic melting)
		Temperature (°C)	ΔC_p (J/g°C)	Temperature (°C)	Temperature (°C)	ΔH (J/g)	
Mannitol:sucrose 3:1	No annealing	-42 ± 0.5	0.1 ± 0.0	-33 ± 0.0	-15 ± 0.2	7.1 ± 0.3	328.1 ± 2.6
	2			-34.5 ± 0.7			332.5 ± 0.7
	8			-33.7 ± 1.1			334.5 ± 0.8
	16			-34.5 ± 0.7			332.8 ± 0.6

607 **Variability in the results are reported in terms of standard deviation (n=3)**

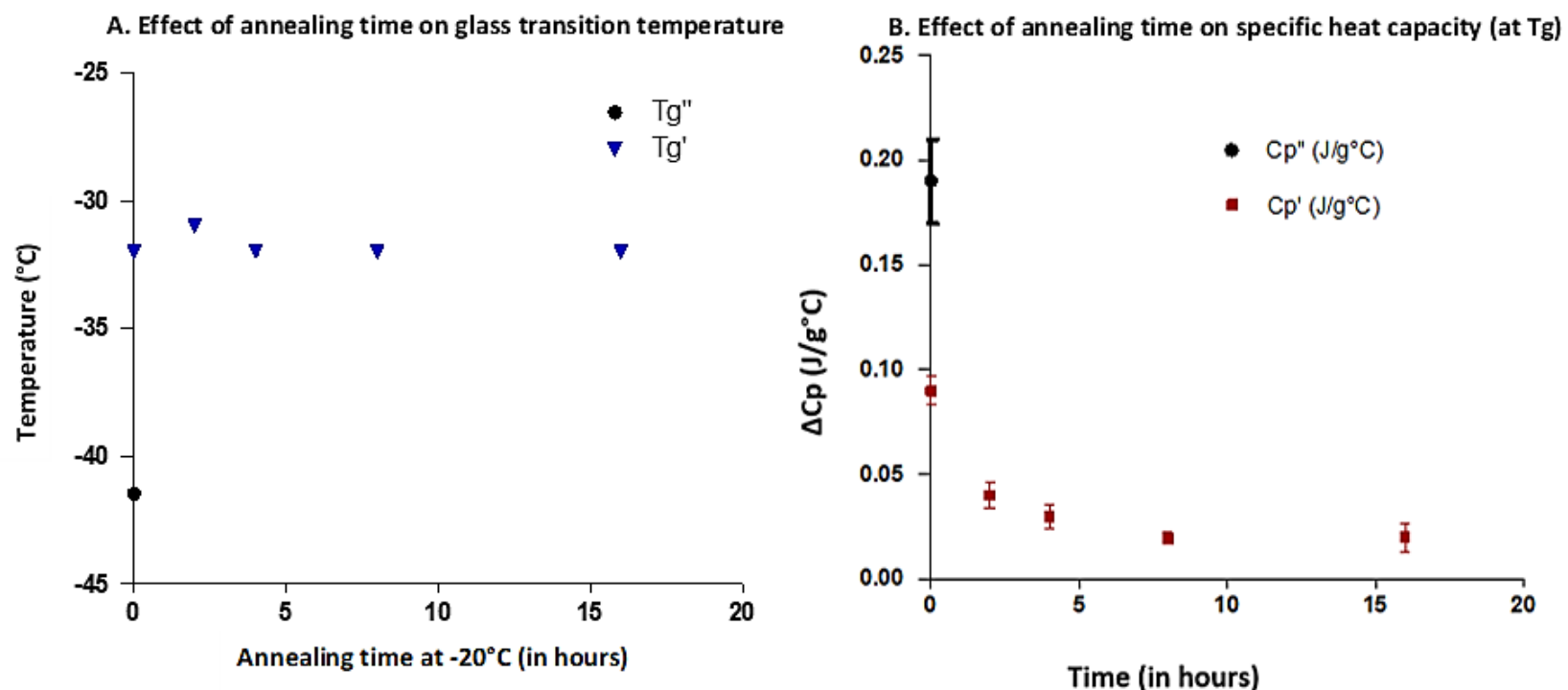
608

609

610

611

612



613

614

Figure 6. Graphical representation for mannitol:trehalose 3:1 (A) Change in glass transition temperature as a function of annealing time at -20°C

(B) Change in heat capacity associated with glass transition temperature as a function of annealing time at -20°C.

615

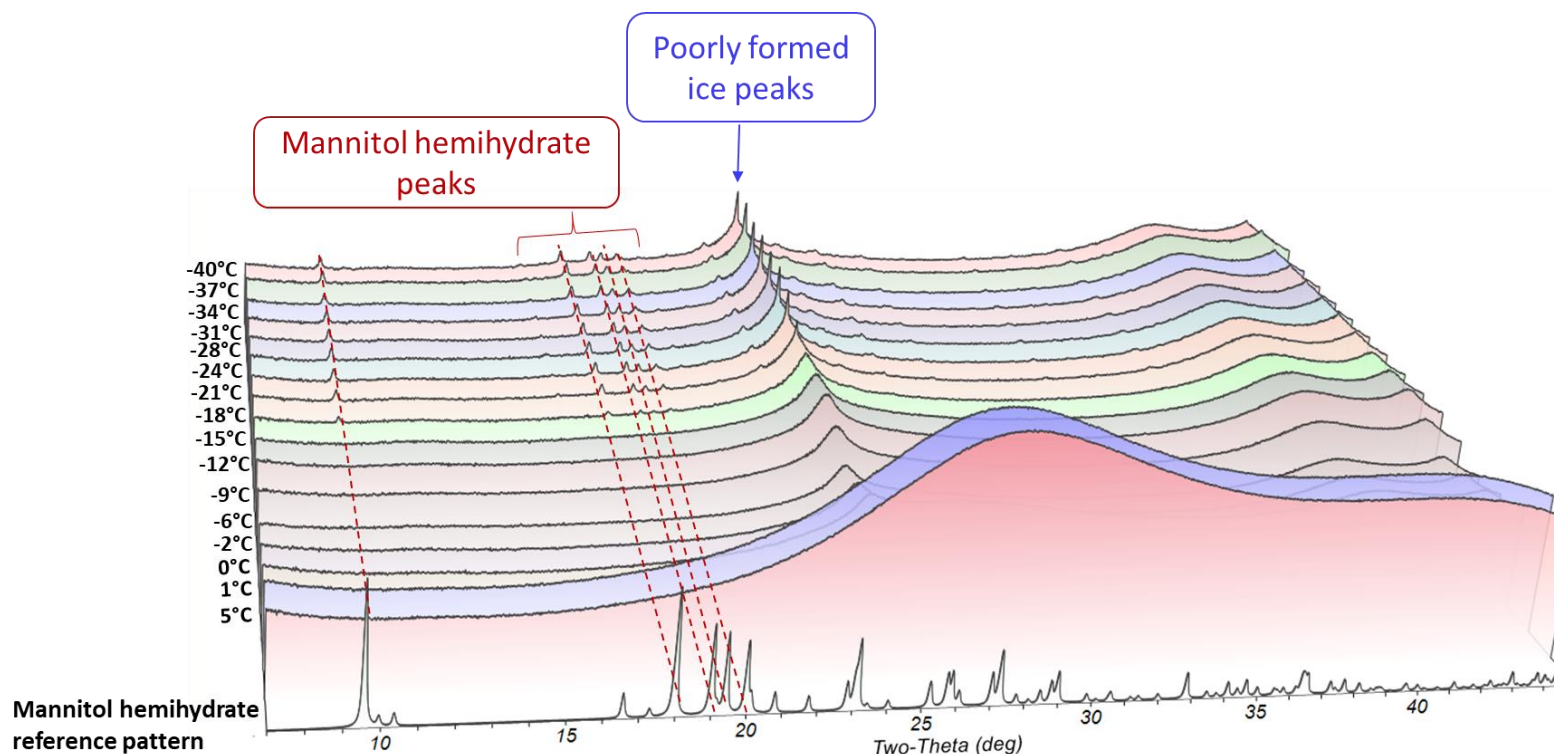
616

617

618

619

620
621
622
623



624 **Figure 7A.** *In situ* synchrotron XRD patterns for mannitol-trehalose (3:1, 5% w/v) solution. Panel A shows overlays of XRD patterns during cooling
625 from 5°C to -40°C; the solution was frozen from room temperature to -45°C at 1°C/min and held at -45°C for 10 minutes followed by heating the
626 samples back to room temperature at 1°C/min. Mannitol hemihydrate reference pattern is shown at the bottom of the overlays. The data were
627 collected using synchrotron radiation (0.45Å). They were converted and plotted for Cu K α radiation (1.54 Å), so as to enable direct comparison
628 with the reference patterns.

629
630
631
632
633
634
635
636
637
638
639
640
641
642
643
644
645
646
647
648
649
650
651
652

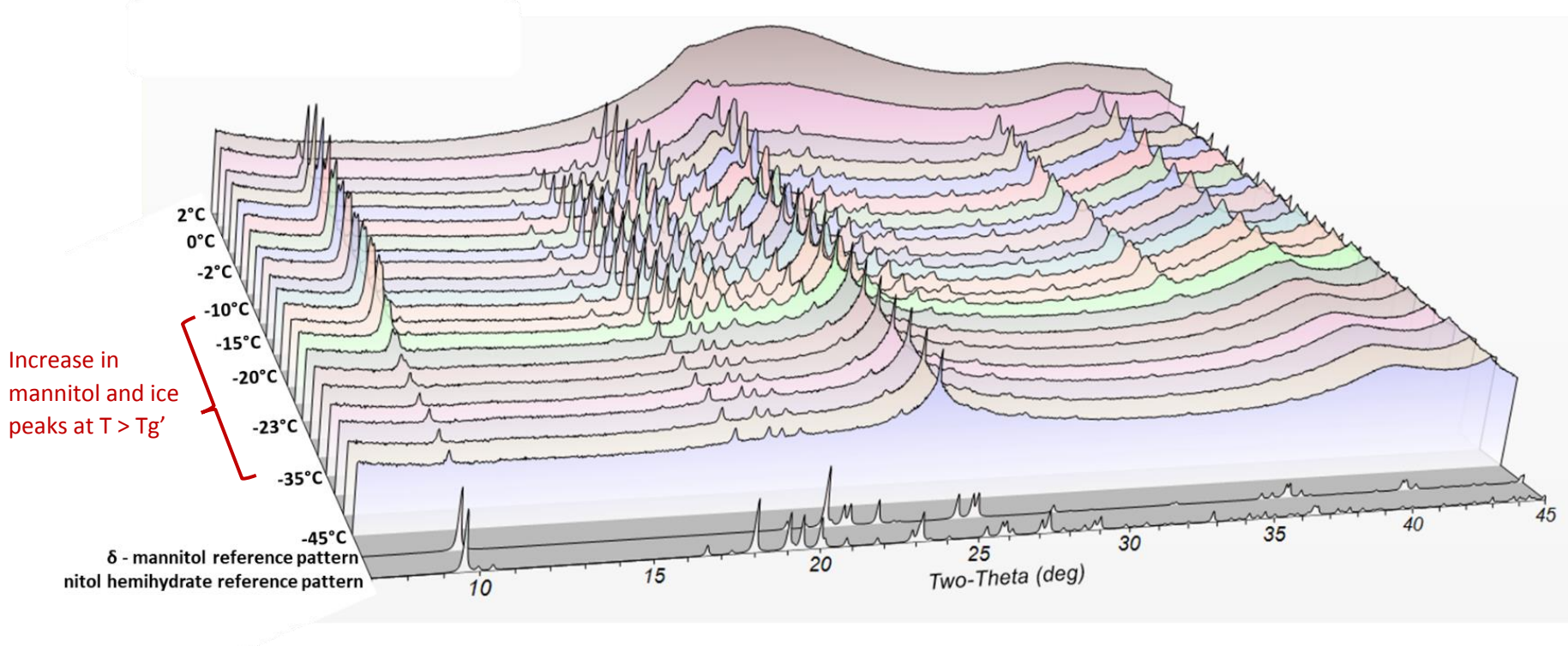
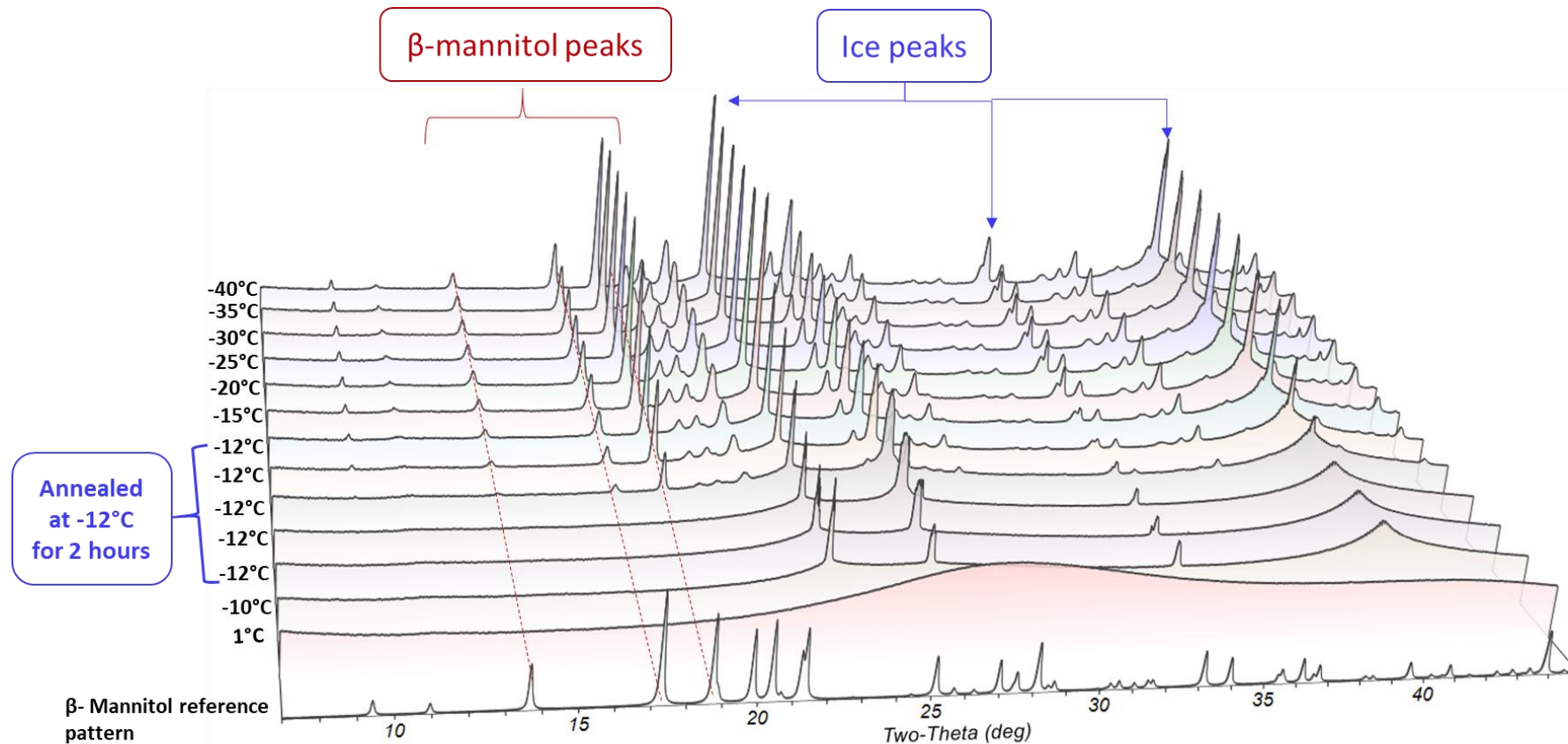


Figure 7B. *In situ* synchrotron XRD patterns for mannitol-trehalose (3:1, 5% w/v) solution. Panel B shows overlays of XRD patterns during heating from -45°C to 2°C at 1°C/min; mannitol hemihydrate and δ -mannitol reference patterns are shown at the bottom of the overlays. The data were collected using synchrotron radiation (0.45 Å). They were converted and plotted for Cu K α radiation (1.54 Å), so as to enable direct comparison with the reference patterns.

653

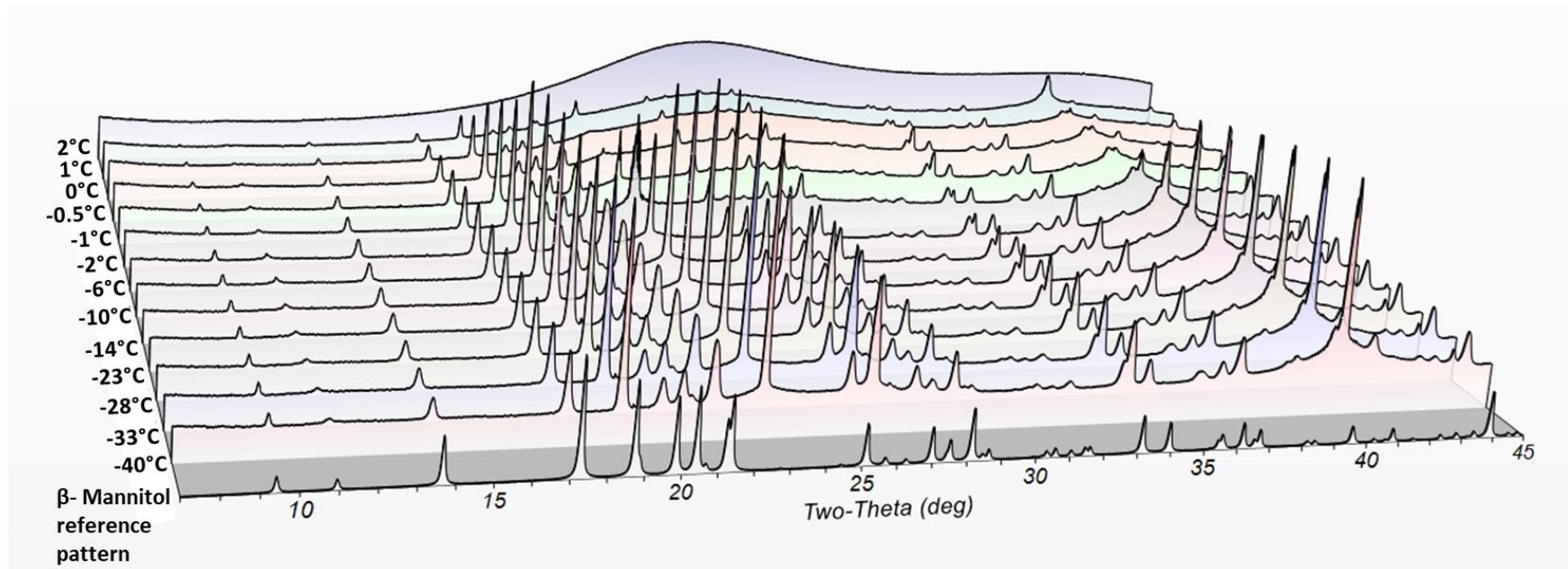
654



655 **Figure 8A.** *In situ* synchrotron XRD patterns for mannitol-trehalose (3:1, 5% w/v) solution during cooling. Panel A shows overlays of XRD patterns
656 during cooling from 5°C to -40°C; mannitol hemihydrate reference pattern is shown at the bottom of the overlays. The solution was frozen from
657 room temperature to -12°C, held for 2 hours further cooled to -45°C at 1°C/min and held at -45°C for 10 minutes. The data were collected using
658 synchrotron radiation (0.45Å). They were converted and plotted for Cu K α radiation (1.54 Å), so as to enable direct comparison with the reference
659 patterns.

660

661



662

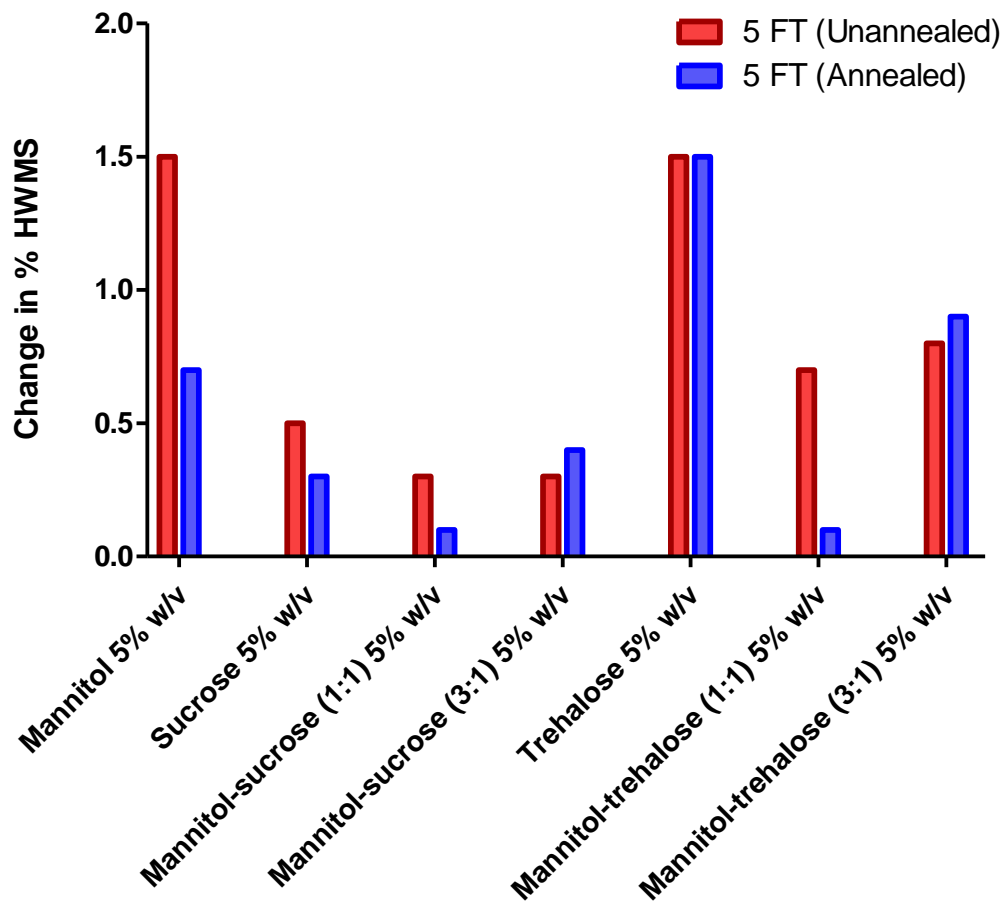
663 **Figure 8B.** *In situ synchrotron XRD patterns for mannitol-trehalose (3:1, 5% w/v) solution during heating. Panel B shows overlays of XRD patterns*

664 *during heating from -45°C to 2°C. The frozen solution was heated from -45°C back to room temperature at 1°C/min. Mannitol hemihydrate and δ-*

665 *mannitol reference patterns are shown at the bottom of the overlays. The data were collected using synchrotron radiation (0.45 Å). They were*

666 *converted and plotted for Cu K α radiation (1.54 Å), so as to enable direct comparison with the reference patterns.*

667
668



669
670
671
672
673
674
675
676
677
678
679
680
681
682

Figure 9. SE-HPLC results for 1 mg/mL HSA with (i) 5% w/w Mannitol (ii) 5% w/w Sucrose (iii) 5% w/w mannitol-sucrose 1:1 (iv) 5% w/w mannitol-sucrose 3:1 (v) 5% w/w Trehalose (vi) 5% w/w mannitol-trehalose 1:1 and (vii) 5% w/w mannitol-sucrose 3:1. The 'change in %HMWS' on the Y-axis refers to the %HMWS in the F/T samples minus the %HMWS in the respective control formulations that were not subjected to 5 F/T cycles. One set of formulations were cooled from room temperature to -45°C and held for 30 minutes at -45°C and reheated back to room temperature at 1°C/min, these formulations were labelled as 'unannealed'. Another set of samples were cooled to -20°C held for 2 hours and further cooled to -45°C and reheated back to room temperature at 1°C/min, these formulations were labelled as 'annealed'.

